EPiC Series in Built Environment

Volume 7, 2026, Pages 505–514

Proceedings of Associated Schools of Construction 62nd Annual International Conference

Early-Age Behavior of Calcium Carbide Residue in Slag-Based Geopolymer Binders

Taofiq Mohammed[1], Mohammad Zunaied Bin Harun[1], and Ebenezer Fanijo[1]
[1]Georgia Institute of Technology

To evaluate the influence of calcium carbide residue (CCR) as a partial slag replacement in geopolymer mortar, binary mixes containing 0–20% CCR were prepared and tested to assess their early-age fresh properties, mechanical performance, microstructural characteristics, and sustainability metrics. Increasing CCR reduced flow (from 133.6 to 83.6 mm) and shortened setting times due to $Ca(OH)_2$ accelerating gel formation. Compressive strength decreased from 9.94 to 6.97 ksi as reactive aluminosilicates were diluted and partial crystallization occurred. XRD of the 20% mix showed C-S-H and portlandite peaks over the amorphous C-A-S-H hump, while SEM revealed a more porous, heterogeneous matrix consistent with strength loss. Environmental analysis showed embodied carbon decreased from 574.6 to 560.6 kg CO_2 e/m³ and material cost dropped ≈6% at 20% CCR. Despite reduced workability and strength, the mixes maintained acceptable performance and improved sustainability compared to OPC mortars. Our results identified an optimal CCR level that balances strength and sustainability, supporting the development of greener, resource-efficient materials.

Keywords: Calcium carbide residue, slag, geopolymer, mortar, sustainability

Introduction

The construction industry seeks sustainable alternatives to ordinary Portland cement (OPC), whose production contributes approximately 7–8% of global CO_2 emissions (Ahmad et al., 2024). In response, geopolymers have emerged as advanced alkali-activated binders synthesized by industrial by-products, offering high mechanical strength, enhanced durability, low permeability, and significantly reduced carbon emissions (Liu et al., 2024; Mohammed, Ul Haq, et al., 2025). In North America, the predominant precursors include Class F fly ash, rich in amorphous aluminosilicates, and ground granulated blast furnace slag (slag), a calcium-rich by-product of steelmaking, both valued for their chemical reactivity and availability (Hanjitsuwan et al., 2018). However, the ongoing reduction in coal-fired power generation and the limited supply of high-quality slag have constrained the consistent production and large-scale deployment of these materials. These limitations have initiated investigation into alternative calcium-rich industrial residues that can provide both alkalinity and reactive calcium to support geopolymerization. Among these, calcium carbide residue (CCR), a by-product of acetylene production, has shown strong potential as a cost-effective, highly alkaline source (Wang et al., 2022). Owing to its high $Ca(OH)_2$ content, CCR can partially or fully substitute conventional chemical activators such as sodium hydroxide (SH) or sodium silicate (SS), thereby lowering material costs, minimizing waste generation, and reducing associated carbon emissions

(Wang et al., 2022). CCR primarily comprises calcium hydroxide ($Ca(OH)_2$) and can act as a solid activator or supplementary precursor in geopolymer systems. When introduced into aluminosilicate-based mixtures, CCR facilitates the formation of calcium silicate hydrate (C-S-H) and calcium aluminosilicate hydrate (C-A-S-H) phases, which coexist with sodium aluminosilicate hydrate (N-A-S-H) gels typical of low-calcium geopolymers, resulting in a denser and stronger matrix (Hanjitsuwan et al., 2018; Phummiphan et al., 2016). Recent research supports CCR's viability in geopolymer and alkali-activated systems. Obeng et al. (2024) extended CCR application to structural-grade geopolymers, showing that metakaolin–CCR blends achieved superior mechanical and bond performance compared to metakaolin-only systems and conventional OPC concretes. Together, these studies demonstrate that CCR is not merely a waste-derived additive, but a reactive calcium source capable of enhancing geopolymer performance across material classes. Despite growing interest in CCR for alkali activation, its role as a partial slag replacement in geopolymer binders remains underexplored. Most prior studies have focused on CCR's activation mechanisms rather than its synergistic interaction with slag or its influence on fresh properties (e.g., flowability and setting time) and microstructural development. Moreover, few efforts have integrated sustainability assessments linking mechanical, microstructural, and environmental performance (Mahmmod & Abbas, 2025). Therefore, this study investigates the effects of 0–20% CCR replacement on the early age fresh and hardened properties along with microstructural behavior of slag-based geopolymer mortar, alongside carbon emission and cost analyses. The goal is to identify an optimal CCR substitution level that balances performance with environmental and economic benefits, advancing the development of sustainable, resource-efficient geopolymer materials.

Materials and Methods

Materials

Slag and CCR were used as the main binders for geopolymer synthesis. The slag, sourced from Argos (Tampa, USA), met the ASTM C989/C989M (2024) specifications, with major oxide constituents of 56.61% CaO, 25.35% SiO2, 8.31% Al2O3. The CCR was supplied by Carbide Industries LLC and GNR Imports Exports (USA). To increase reactive CaO content, CCR was thermally processed before use. The residue was air-dried for 24 h, oven-dried at 110 °C for 2 h, then pulverized and sieved through a 150 µm mesh to obtain a fine, homogeneous powder suitable for geopolymerization. The processed CCR was highly alkaline, containing mainly CaO (96.43%) with minor SiO_2 (1.45%) and Al_2O_3 (1.12%). **Figure 1** show the particle morphology: CCR exhibited irregular, porous particles typical of crystalline portlandite, while slag showed angular, glassy particles with smoother surfaces. XRF results for both precursors are given in **Table 1**. Commercial-grade SH (pellets, 97% purity) and SS (14.7% Na_2O, 29.4% SiO_2, 55.9% H_2O; $SiO_2/Na_2O \approx 2.0$) from Sigma-Aldrich were used as alkali activators.

Figure 1. SEM micrograph of (a) CCR, and (b) Slag.

Table 1. Chemical composition of the precursors

Oxides (%)	SiO_2	Al_2O_3	CaO	MgO	SO_3	TiO_2	Na_2O	K_2O	Fe_2O_3	P_2O_5
Slag	25.35	8.31	56.61	3.07	4.7	0.86	0	0.41	0.69	0
CCR	1.45	1.12	96.43	0.18	0.07	0.11	0.23	0	0.23	0.18

Mix Proportions and Preparation

To investigate the effect of CCR on slag-based geopolymer properties, five mixes were prepared by partially replacing slag with CCR at 0%, 5%, 10%, 15%, and 20% by weight of total binder. The alkali activator-to-binder (A/B) ratio of 0.4 was used based on previous studies (Ghafoor et al., 2021) and SS/SH of 2.5 (Arafa et al., 2018), while 1.6 was used as the sand-to-binder ratio (S/B) (Hanjitsuwan et al., 2017). 10 M SH solution was prepared 24 hours prior and allowed to cool before mixing with SS. The binders were mixed thoroughly for 5 mins before mixing with sand for another 5 mins after which the pre-prepared alkaline solution was gradually incorporated. Mixing continued for an additional 5 mins until a uniform mortar was achieved. The fresh geopolymer mortar was immediately cast into 2in cube molds in two layers, each tamped 20 times to compact and remove entrapped air. The specimens were covered with thin polyethylene films to minimize evaporation. The specimens were demolded 24 h after casting and subsequently sealed in polyethylene bags to maintain moisture before curing at ambient temperature in a controlled chamber for 7 days. Summary of the mix design is provided in **Figure 2**, and the experimental workflow is shown in **Figure 3**.

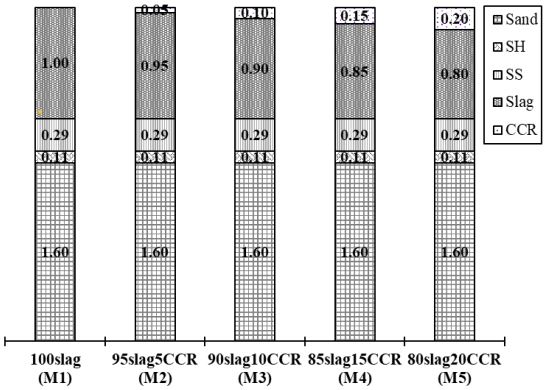

Figure 2. Mix design proportion of M1 to M5

Testing Methods

After preparing the fresh geopolymer mortar, the flowability of each mix was determined in accordance with ASTM C1437 (2020) using a standard flow table. A truncated cone mold (4 in base, 2.75 in top, 2 in height) was filled in two layers, tamped 20 times, lifted, and the flow table dropped 25 times in 15 s. The average spread from four measurements was recorded as the flow value. Initial and final setting times were determined per ASTM C807 (2021) using a modified Vicat apparatus. Fresh mortar was placed in a Vicat mold, and penetration resistance was monitored until reaching 10 mm (initial set) and 0 mm (final set). Compressive strength was measured after 7 days of curing using a Humboldt HCM-300iHAC compression machine following (ASTM C109, 2024). The average of

three specimens was reported for each mix. Two mixes, M1 (control, pure slag) and M5 (highest CCR level), were selected for microstructural and phase analysis. XRD was performed using a Rigaku Miniflex (Cu-Kα, 40 kV, 30 mA) over a 2θ range of 10–70° at 1°/min. SEM analysis using a Thermo Axia Variable Pressure SEM examined surface morphology and elemental composition. Hardened paste fragments were epoxy-impregnated, then ground and polished with progressively finer silicon carbide papers on a Struers Rotopol-15 system. The embodied carbon footprint (ECF) of our mixes was estimated using a cradle-to-gate approach limited to module A1 (raw-material supply), with a functional unit of 1 m³ of fresh mortar. Carbon emission factors (kg CO_2 e/kg) used in this study were obtained from literature as follows: CCR = 0.083 (Anandan Govindan et al., 2025), Slag = 0.155 (Heidelberg Materials, 2025), Sand = 0.0139 (Setiawan et al., 2023), SH = 1.915 (Turner & Collins, 2013), and SS = 0.6813 (Setiawan et al., 2023). CCR has an allocated emission of 0.083 kg CO_2 e/kg (Anandan Govindan et al., 2025), though some studies treat it as a by-product with zero emissions (Mahmmod & Abbas, 2025). For slag, reported values range from 0.08 kg CO_2 e/kg (Casey, 2025) to 0.155 kg CO_2 e/kg when economic allocation for co-products is applied (Heidelberg Materials, 2025). The mix impact was calculated as

$$ECF = \sum (M(i) \times UnitMCO_2\, e) \quad (1)$$

Where, ECF = Embodied carbon footprint, kg CO_2 e/m^3; M(i) = Quantity of each ingredient, i (i.e. Slag, SH, SS, sand and CCR) in the mortar mixture for 1m^3 of mortar production, kg; and UnitMCO_2 e = Cradle-to-gate (A1-A3) carbon emissions allocated, kgCO_2 e/kg.

For the economic analysis, the total cost of each mix was estimated by combining the mix proportions with current market prices for all materials. CCR was assigned zero cost due to its minimal processing requirements (Mahmmod & Abbas, 2025).

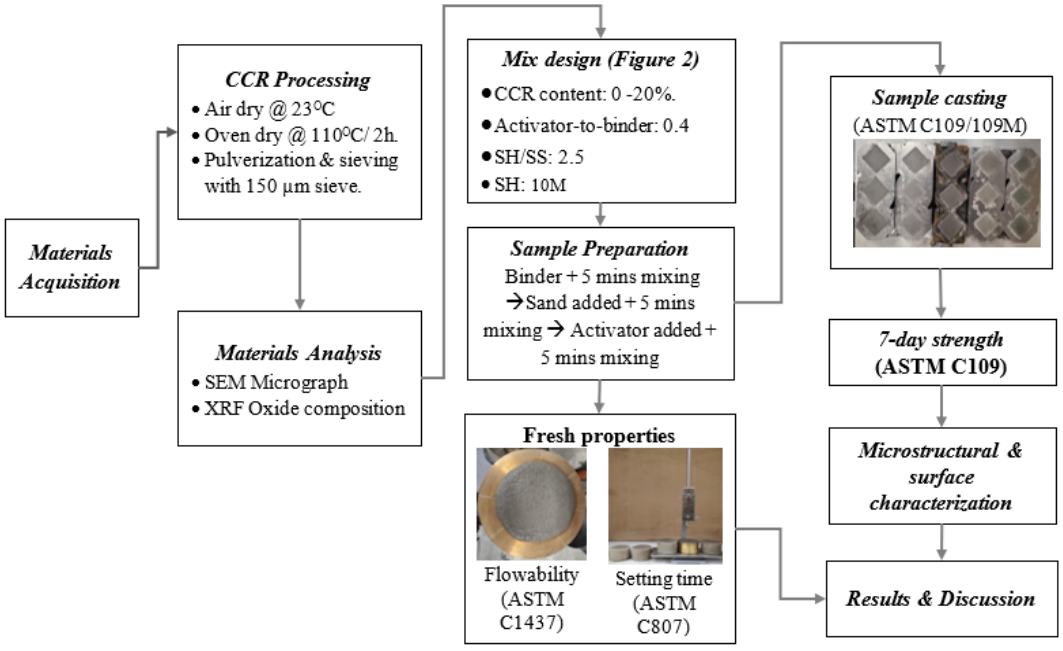

Figure 3. Schematic flow chart of sample preparation and testing procedure.

Results and discussion

Flowability

The flowability of the geopolymer sample decreased gradually with increasing CCR content, as shown in **Figure 4(a)**. Flowability decreased by 37% with higher CCR content, indicating reduced workability. The M3 mix (115.6 mm) was closest to the ASTM C1437 optimum (110 ± 5 mm), suggesting 10% CCR offers the best balance. Mixes above 120 mm were overly fluid, while those below 100 mm were stiff due to CCR's fine particles increasing water demand and early gel formation. This decline in flowability can be attributed primarily to the high surface area and fineness of CCR, which increases water demand and accelerates the geopolymerization reaction (Phummiphan et al., 2016). Furthermore, CCR particles have a rough, irregular morphology that enhances interparticle friction and limits paste fluidity, consistent with the microstructural observations reported by Hanjitsuwan et al. (2018).

Setting time

The initial and final setting times of the geopolymer sample decreased progressively as the CCR content increased, as shown in **Figure 4(b)**. The observed acceleration in setting with increasing CCR content can be attributed to the high concentration of $Ca(OH)_2$ present in CCR, which provides additional calcium ions (Ca^{2+}) that promote early geopolymerization and rapid gel formation (Sun et al., 2023). The increased availability of calcium facilitates the coexistence of C-S-H and C-A-S-H gels alongside the typical N-A-S-H structure of slag-based geopolymers. This dual gel formation accelerates setting by rapidly consuming dissolved silicate and aluminate species (Phummiphan et al., 2016). A similar trend was reported by Hanjitsuwan et al. (2018), Phoo-ngernkham et al. (2020) and Obeng et al. (2023). While faster setting promotes early strength, excessive acceleration in higher CCR mixes reduces workable time. An optimal CCR level is thus required to balance setting and workability; in this study, 10% CCR (M3) achieved this balance with initial and final setting times of 18 and 28 minutes.

Compressive Strength

As shown in **Figure 4a**, the 7-day compressive strength results show a progressive decline with increasing CCR content, from 9.94 ksi (M1) and 9.01 ksi (M2) to 6.97 ksi (M5). This reduction is mainly attributed to the dilution of reactive aluminosilicate phases and the slower dissolution rate of CCR compared to slag. Since CCR is predominantly composed of $Ca(OH)_2$, it reacts less efficiently with the alkaline activator than the amorphous slag phases, resulting in reduced gel formation and lower strength (Hanjitsuwan et al., 2018). Beyond 10% CCR, strength loss became pronounced as excess calcium and low aluminosilicate content disrupted the optimal Si/Al ratio for geopolymerization (Phoo-ngernkham et al., 2020). This imbalance favors the precipitation of crystalline calcium-rich phases rather than the development of a continuous amorphous gel, leading to a more porous microstructure (Phummiphan et al., 2016; Obeng, et al., 2024; Mohammed, Singh, et al., 2025). Despite the reduction, all mixes (**Table 2**) still achieved strengths between 6.97 and 9.94 ksi (48 – 69 MPa) after 7 days, values that are comparable to or higher than those typically attained by conventional OPC concretes at the same age.

Table 2. 7-day strength of the geopolymer mixes (Mean ± STD)

Mixes	**M1**	**M2**	**M3**	**M4**	**M5**
7-day strength (ksi)	9.94 ± 0.64	9.01 ± 0.45	8.04 ± 0.54	7.77 ± 0.60	6.97 ± 0.13

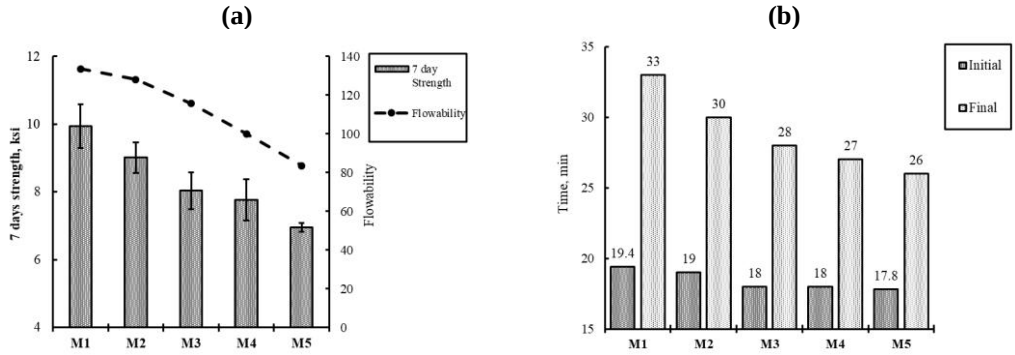

Figure 4. (a) Flowability and 7-day strength, (b) Initial and final setting time of mixes

XRD Crystallographic Analysis

The 7-day XRD patterns of M1 and M5 geopolymer mixes (**Figure 5**) revealed a dominant broad hump between 20°–35° 2θ centered near 29.4°, characteristic of amorphous C-A-S-H gel, the main binding phase in alkali-activated slag systems. Both mixes also showed a calcite peak near 29.4°, likely from carbonation or residual slag content. However, M5 exhibited additional sharp peaks at 20.8°, 26.5°, and 36.3°, corresponding to semi-crystalline C-S-H and portlandite phases, confirming partial crystallization due to excess calcium from CCR. This increased Ca^{2+} availability accelerates early gel formation but disrupts the Si/Al framework, promoting discrete crystalline domains instead of a uniform amorphous network (Obeng, et al., 2024; Wang et al., 2022). The resulting heterogeneous and porous matrix explains the lower compressive strength of M5 compared to the fully amorphous M1, aligning with similar observations in previous studies (Hanjitsuwan et al., 2018; Phummiphan et al., 2016).

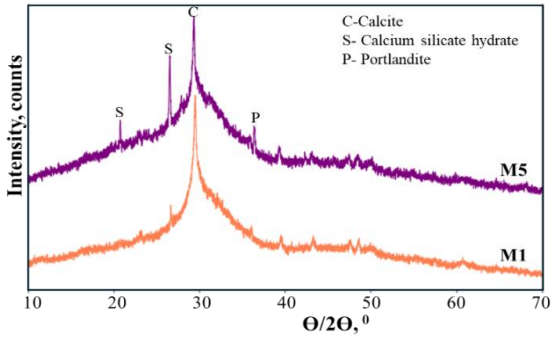

Figure 5. XRD patterns confirming CCR-induced partial crystallization

SEM Surface Micrograph Result

The 7 days SEM micrographs of the M1 and M5 geopolymer samples are shown in **Figure 6**. M1 presents a relatively dense and compact matrix with fewer unreacted slag particles, indicating effective C-A-S-H gel formation (Chen et al., 2025; Zhang et al., 2025). M3 shows a less compact and more porous microstructure, with a greater number of partially or unreacted slag particles, incompletely reacted CCR, and more extensive cracking. These features indicate incomplete geopolymerization and weaker particle bonding (Chen et al., 2025). These morphological features are consistent with the observed reduction in compressive strength. While CCR addition supplied reactive

calcium that promoted early gel nucleation, it also produced a less uniform and more porous microstructure, creating stress points and lowering strength. Hanjitsuwan et al. (2018) similarly reported that excess CCR caused rapid C-S-H and portlandite precipitation, leading to microcracking and reduced long-term strength.

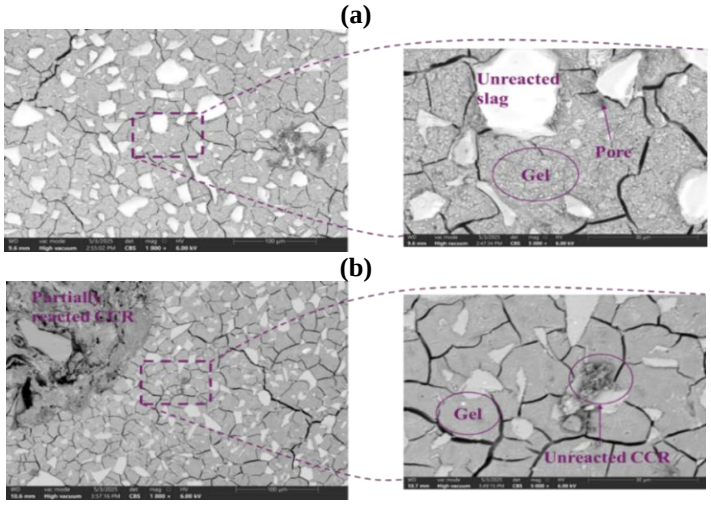

Figure 6. SEM at 7 days: (a) M1 shows a dense matrix with minor pores; (b) M5 shows a porous, heterogeneous structure with partially reacted CCR

Environmental and economic analysis

The environmental impact of different geopolymer mortar blends was evaluated through the ECF (*kg CO_2 e/m^3*) for each of the mixtures. **Figure 7** summarizes the ECF of mortar blends studied in this study. From **Figure 7(a)** it can be observed that, as CCR incrementally replaces slag from 0% to 20% of binder, the total ECF drops linearly from 574.6 to 560.6 CO_2 e/m^3, a reduction of 2.4% takes place. Although, the substitution of slag with CCR brings down the embodied carbon footprint very marginally, it can be postulated that the use of CCR as a partial precursor is a viable option as the amount of slag is getting limited due the regulation on steel production. **Figure 8** shows the effect of replacing slag with CCR on the relative production cost of geopolymer mortar considering only the value of slag, CCR and sand. It can be observed that a 6% cost can be reduced by replacing 20% slag by CCR.

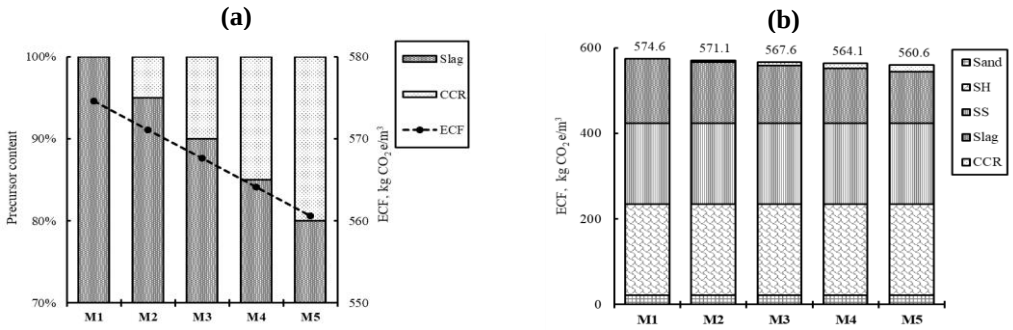

Figure 7. Embodied carbon footprint for mixes studied (a) changes with CCR replacement %, (b) contribution of different constituent materials to ECF

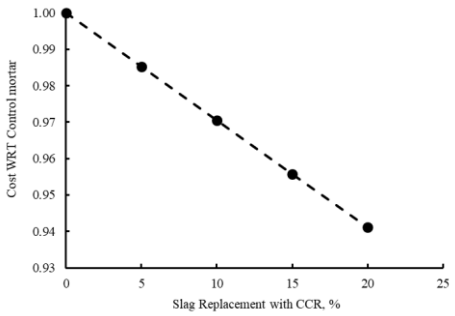

Figure 8. Effect of slag replacement with CCR on relative cost of mortar

Results and discussion

This study investigated the early age performance of CCR as a supplementary precursor in slag-based geopolymer mortar. Based on the experimental results, the following conclusions are drawn:

1. Fresh properties: Increasing CCR content slightly reduced flowability due to higher fineness and water demand; however, all mixes remained near the ASTM C1436 workability limit. M3 showed the best balance between flow and cohesion. Setting times decreased modestly with higher CCR, attributed to increased calcium availability accelerating polycondensation, while all mixes retained rapid-setting behavior suitable for precast and repair applications.
2. Mechanical performance: Strength decreased from 9.94 ksi in M1 to 6.97 ksi in M5 (~30% reduction), primarily due to dilution of reactive aluminosilicates and increased CaO promoting crystalline C-S-H over amorphous C-A-S-H gel formation. Nevertheless, all mixes achieved strengths comparable to or exceeding OPC mortars at the same age.
3. Microstructural evolution: XRD revealed a shift from a predominantly amorphous matrix in the control to a hybrid amorphous-crystalline structure with CCR inclusion, evidenced by C-S-H, calcite, and portlandite peaks in M5. SEM confirmed a transition from a dense, continuous gel to a more porous, heterogeneous matrix with unreacted CCR particles, explaining the observed strength reduction.
4. Environmental and cost impact: Replacing slag with 0–20% CCR reduced total ECF linearly from 574.6 to 560.6 kg CO_2e/m^3 (−2.4%) and achieved up to a 6% cost reduction at 20% CCR. Despite ECF gains, CCR remains a viable alternative given constrained slag availability from steel-production regulations. Further research will include long-term durability studies under aggressive exposure conditions to further validate the practical potential of CCR in slag based geopolymer mortar.

References

Ahmad, M. R., Fernàndez-Jimenez, A., Chen, B., Leng, Z., & Dai, J. G. (2024). Low-carbon cementitious materials: Scale-up potential, environmental impact and barriers. *Construction and Building Materials*, 455. https://doi.org/10.1016/j.conbuildmat.2024.139087

Anandan Govindan, S., Mudavath, H., & Vaddemani, G. P. R. (2025). Evaluating the sustainability of using calcium carbide residue for clay stabilization: integrating mechanical behaviour and life cycle assessment. *Environmental Science and Pollution Research*, 32(26), 15772–15789. https://doi.org/10.1007/s11356-025-36608-9

Arafa, S. A., Ali, A. Z. M., Awal, A. S. M. A., & Loon, L. Y. (2018). Optimum mix for fly ash geopolymer binder based on workability and compressive strength. *IOP Conference Series: Earth and Environmental Science*, 140(1). https://doi.org/10.1088/1755-1315/140/1/012157

ASTM C109. (2024). *Test Method for Compressive Strength of Hydraulic Cement Mortars (Using 50mm [2 in.] Cube Specimens)*. ASTM International. https://doi.org/10.1520/C0109_C0109M-24

ASTM C807. (2021). *Test Method for Time of Setting of Hydraulic Cement Mortar by Modified Vicat Needle*. ASTM International. https://doi.org/10.1520/C0807-21

ASTM C989/C989M. (2024). *Specification for Slag Cement for Use in Concrete and Mortars*. ASTM International. https://doi.org/10.1520/C0989_C0989M-24

ASTM C1437. (2020). *Test Method for Flow of Hydraulic Cement Mortar*. ASTM International. https://doi.org/10.1520/C1437

Casey, D. (2025). *Embodied CO2 e of UK cements*. https://share.mediaflow.com/

Chen, M., Wu, D., Chen, K., Liu, C., Zhou, G., & Cheng, P. (2025). The effects of solid activator dosage and the liquid-solid ratio on the properties of FA-GGBS based one-part geopolymer. *Construction and Building Materials*, 463. https://doi.org/10.1016/j.conbuildmat.2025.140067

Ghafoor, M. T., Khan, Q. S., Qazi, A. U., Sheikh, M. N., & Hadi, M. N. S. (2021). Influence of alkaline activators on the mechanical properties of fly ash based geopolymer concrete cured at ambient temperature. *Construction and Building Materials*, 273. https://doi.org/10.1016/j.conbuildmat.2020.121752

Hanjitsuwan, S., Phoo-ngernkham, T., & Damrongwiriyanupap, N. (2017). Comparative study using Portland cement and calcium carbide residue as a promoter in bottom ash geopolymer mortar. *Construction and Building Materials*, 133, 128–134. https://doi.org/10.1016/j.conbuildmat.2016.12.046

Hanjitsuwan, S., Phoo-ngernkham, T., Li, L. yuan, Damrongwiriyanupap, N., & Chindaprasirt, P. (2018). Strength development and durability of alkali-activated fly ash mortar with calcium carbide residue as additive. *Construction and Building Materials*, 162, 714–723. https://doi.org/10.1016/j.conbuildmat.2017.12.034

Heidelberg Materials. (2025). *Environmental product declaration - Heidelberg Materials UK* – UK Average Regen GGBS.

Liu, X., Xiao, G., Yang, D., Dai, L., & Tang, A. (2024). Sustainable Cementitious Materials: Strength and Microstructural Characteristics of Calcium Carbide Residue-Activated Ground Granulated Blast Furnace Slag–Fly Ash Composites. *Sustainability (Switzerland)*, 16(24). https://doi.org/10.3390/su162411168

Mahmmod, L. M. R., & Abbas, W. A. (2025). Potential impact of calcium carbide residue on the fresh and hardened behavior of eco-friendly cement-based composites. *Cleaner Waste Systems*, 11. https://doi.org/10.1016/j.clwas.2025.100307

Mohammed, T. O., Singh, D., & Fanijo, E. O. (2025). Calcium Carbide Residue as a Supplementary Precursor is Geopolymer Binders. *Frontiers in Materials*, 12. https://doi.org/10.3389/fmats.2025.1718575

Mohammed, T. O., Ul Haq, A., Harun, M. Z. Bin, & Fanijo, E. O. (2025). Recent Advances in Fly Ash- and Slag-Based Geopolymer Cements. *Sustainability*, 17(24), 11167. https://doi.org/10.3390/su172411167

Obeng, J., Andrews, A., Adom-Asamoah, M., & Adjei, S. (2023). Effect of calcium carbide residue on the sulphate resistance of metakaolin-based geopolymer mortars. *Cleaner Materials*, 7. https://doi.org/10.1016/j.clema.2023.100177

Obeng, J., Andrews, A., Adom-Asamoah, M., & Owusu-Twumasi, J. (2024). Bond behavior of reinforcing steel bars in metakaolin - calcium carbide residue-based geopolymer concrete. *Engineering Research Express*, 6(3). https://doi.org/10.1088/2631-8695/ad722b

Phoo-ngernkham, T., Phiangphimai, C., Intarabut, D., Hanjitsuwan, S., Damrongwiriyanupap, N., Li, L. yuan, & Chindaprasirt, P. (2020). Low cost and sustainable repair material made from alkali-activated high-calcium fly ash with calcium carbide residue. *Construction and Building Materials*, 247. https://doi.org/10.1016/j.conbuildmat.2020.118543

Phummiphan, I., Horpibulsuk, S., Phoo-ngernkham, T., Arulrajah, A., & Shen, S.-L. (2016). Marginal Lateritic Soil Stabilized with Calcium Carbide Residue and Fly Ash Geopolymers as a Sustainable Pavement Base Material. *Journal of Materials in Civil Engineering*, 29(2). https://doi.org/10.1061/(ASCE)MT

Setiawan, A. A., Hardjasaputra, H., & Soegiarso, R. (2023). Embodied carbon dioxide of fly ash based geopolymer concrete. IOP Conference Series: *Earth and Environmental Science*, 1195(1), 012031. https://doi.org/10.1088/1755-1315/1195/1/012031

Sun, D., Yin, F., Deng, Y., Liu, K., Tang, J., Shen, C., Sun, Y., Wang, A., Huang, N., & Hu, C. (2023). Utilization of carbide slag in autoclaved aerated concrete (CS-AAC) and optimization: Foaming, hydration process, and physic-mechanical properties. *Case Studies in Construction Materials*, 19. https://doi.org/10.1016/j.cscm.2023.e02354

Turner, L. K., & Collins, F. G. (2013). Carbon dioxide equivalent (CO2-e) emissions: A comparison between geopolymer and OPC cement concrete. *Construction and Building Materials*, 43, 125–130. https://doi.org/10.1016/j.conbuildmat.2013.01.023

Wang, Q., Guo, H., Yu, T., Yuan, P., Deng, L., & Zhang, B. (2022). Utilization of Calcium Carbide Residue as Solid Alkali for Preparing Fly Ash-Based Geopolymers: Dependence of Compressive Strength and Microstructure on Calcium Carbide Residue, Water Content and Curing Temperature. *Materials*, 15(3). https://doi.org/10.3390/ma15030973

Zhang, P., Mao, Y., Gao, Z., Guo, J., & Zheng, M. (2025). Efficient utilization of waste drilling mud to prepare material stabilized with fly ash/slag based geopolymer for subgrade engineering. *Journal of Environmental Management*, 373. https://doi.org/10.1016/j.jenvman.2024.123600